hnRNP K post-transcriptionally co-regulates multiple cytoskeletal genes needed for axonogenesis

Yuanyuan Liu and Ben G. Szaro*

SUMMARY

The RNA-binding protein, hnRNP K, is essential for axonogenesis. Suppressing its expression in *Xenopus* embryos yields terminally specified neurons with severely disorganized microtubules, microfilaments and neurofilaments, raising the hypothesis that hnRNP K post-transcriptionally regulates multiple transcripts of proteins that organize the axonal cytoskeleton. To identify downstream candidates for this regulation, RNAs that co-immunoprecipitated from juvenile brain with hnRNP K were identified on microarrays. A substantial number of these transcripts were linked to the cytoskeleton and to intracellular localization, trafficking and transport. Injection into embryos of a non-coding RNA bearing multiple copies of an hnRNP K RNA-binding consensus sequence found within these transcripts largely phenocopied hnRNP K knockdown, further supporting the idea that it regulates axonogenesis through its binding to downstream target RNAs. For further study of regulation by hnRNP K of the cytoskeleton during axon outgrowth, we focused on three validated RNAs representing elements associated with all three polymers – Arp2, tau and an α-internexin-like neurofilament. All three were co-regulated post-transcriptionally by hnRNP K, as hnRNP K knockdown yielded comparable defects in their nuclear export and translation but not transcription. Directly knocking down expression of all three together, but not each one individually, substantially reproduced the axonless phenotype, providing further evidence that regulation of axonogenesis by hnRNP K occurs largely through pleiotropic effects on cytoskeletal-associated targets. These experiments provide evidence that hnRNP K is the nexus of a novel post-transcriptional regulatory module controlling the synthesis of proteins that integrate all three cytoskeletal polymers to form the axon.

KEY WORDS: Microtubule associated protein tau, Actin-related protein 2, α-Internexin, *Xenopus laevis*

INTRODUCTION

Control of expression of proteins associated with the cytoskeleton is crucial for meeting changing demands for structural materials as axonal growth shifts between bouts of extension, pausing, retraction and branching. Not only must the total amount of protein available be appropriate to sustain growth, but also the relative abundance among constituents of the three polymers must be kept in balance. For example, imbalances among Type IV neurofilament (NF) subunits lead to pathogenic aggregates (Lariviére and Julien, 2004), and overexpression of the microtubule associated protein tau relative to NFs induces premature retraction of developing neurites (Dubey et al., 2008). For NFs, studies of developing mammalian neurons and regenerating *Xenopus* optic axons have demonstrated that this control involves an interplay between modulations in gene transcription and post-transcriptional control of nuclear export, turnover and translation of the RNAs (Ananthakrishnan et al., 2008; Ananthakrishnan and Szaro, 2009; Moskowitz and Oblinger, 1995; Schwartz et al., 1994). Whether such interplay extends to other cytoskeletal constituents and how expression is coordinated among them is unknown.

Ribonucleoproteins (RNPs) that bind NF mRNAs have a major role in directing their expression (Lin and Schlaepfer, 2006; Szaro and Strong, 2010). One such RNP, hnRNP K, binds all three NF

triplet RNAs (Thyagarajan and Szaro, 2004; Thyagarajan and Szaro, 2008). It is a member of a family of triple K-homology (KH) RNA-binding domain RNPs, which includes hnRNPs E1 and E2 and the Nova RNA-binding proteins (Buckanovich et al., 1993; Buckanovich et al., 1996; Lewis et al., 1999; Nakagawa et al., 1986). Although hnRNP K is abundantly expressed in neurons (Blanchette et al., 2006; Liu et al., 2008; Thyagarajan and Szaro, 2004), its cellular functions are known mostly from studies in cell lines, which indicate that it shuttles between the nucleus and cytoplasm and participates in multiple aspects of RNA metabolism, from splicing and nuclear export to translation and turnover. As the substrate of numerous kinases, hnRNP K is ideally suited for coupling the fates of its RNA targets with cell signaling (Adolph et al., 2007; Collier et al., 1998; Habelhah et al., 2001; Mikula et al., 2006; Ostareck-Lederer et al., 2002). Current models propose that hnRNP K is a scaffolding protein, controlling its target RNAs through combinatorial interactions with multiple partners, which can either bind hnRNP K directly, depending on its phosphorylation state, or interact indirectly through steric hindrance and competition while binding (Bomsztyk et al., 1997; Bomsztyk et al., 2004; Makeyev and Liebhaber, 2002; Ostareck et al., 1997; Ostareck-Lederer et al., 1998).

In developing *Xenopus* neurons, hnRNP K plays an essential role in regulating the nuclear export and translation of the middle NF triplet (*NF-M*) subunit's mRNA (Liu et al., 2008). In these neurons, hnRNP K knockdown also leads specifically to a cell-autonomous failure of axons to develop, without significantly affecting either neural pattern formation or terminal neuronal specification (Liu et al., 2008). Because loss of NF-M by itself is insufficient to account for a complete failure of axons to develop (Hirokawa and Takeda, 1999; Lin and Szaro, 1996; Walker et al., 2001), hnRNP K must

Department of Biological Sciences and the Center for Neuroscience Research, University at Albany, SUNY, Albany, NY 12222, USA.

*Author for correspondence (bgs86@albany.edu)

post-transcriptionally regulate additional transcripts used to make the axon. The current study tests this hypothesis by demonstrating that hnRNP K plays its crucial role in axon outgrowth, downstream of neuronal specification and the initial establishment of cell polarity, by functioning as an RNA-binding protein that co-regulates the expression of multiple transcripts. In large part, these transcripts include components associated with microtubules, microfilaments and neurofilaments that collectively organize these polymers into an axon.

MATERIALS AND METHODS
Microinjection and culturing of embryos
Antisense morpholino oligonucleotides (MOs; Gene Tools) to Arp2, tau and XNIF targeted nucleotides –50 to –27, –52 to –28, and +1 to +25, respectively. The hnRNP K MO (#1) and control MO were described previously (Liu et al., 2008). For non-coding RNAs, sense and antisense oligonucleotides (see Table S1 in the supplementary material) with *Not*I overhangs were synthesized (Integrated DNA Technologies) and ligated after annealing into a modified pGem3Z expression vector (Lin and Szaro, 1996). After clones were sequenced to confirm their correctness (GENEWIZ), they were linearized with *Xho*I for in vitro transcription of 7-methyl-guanosine-capped RNA (mMESSAGE mMACHINE SP6; Ambion). hnRNP K RNA lacking the MO-targeting sequence was prepared as described (Liu et al., 2008).

One (unilateral) or both (bilateral) blastomeres of two-cell, periodic albino *Xenopus laevis* embryos were microinjected with MO (single MO, 10 nl of 1 ng/nl; three MOs, 5 nl of 1 ng/nl each) or in vitro transcribed RNA (10 nl of 1 ng/nl) mixed with fluorescent dextrans (0.75% w/v lysinated FITC-Dextran, Molecular Probes) or enhanced green fluorescent protein RNA (200 pg) as described (Gervasi and Szaro, 2004; Liu et al., 2008). Rescue from hnRNP K MO (10 ng) was carried out by co-injecting hnRNP K RNA lacking the MO-target sequence (100 pg) as described (Liu et al., 2008). Dissociated embryonic spinal cord/hindbrain-myotomal cultures were prepared from stage 22 embryos (one per culture) as described (Tabti and Poo, 1991; Undamatla and Szaro, 2001).

Immunological procedures
Primary antibodies (#1-5, mouse monoclonal; #6-10, rabbit antisera; #11, goat antiserum) were directed against: (1) hnRNP K, 1:100 (clone 3C2; Santa Cruz Biotechnology); (2) *Xenopus* NF-M, 2 μg/ml (RMO270); (3) a *Xenopus* neuronal β-tubulin (N-β tubulin) isotype, 1:100 (clone JDR.38B; Sigma); (4) actin related protein 2 (Arp2), 1:200 (clone E2, Santa Cruz); (5) glyceraldehyde phosphate dehydrogenase (GAPDH), 5 μg/ml (clone 6C5; Ambion); (6) the conserved carboxy terminal region of tau (tau-3′), 1:2000; (7) *Xenopus* peripherin, 1:2000; (8) a *Xenopus* α-internexin-like NF (XNIF), 1:500; (9) partitioning defective 3 homolog (Par3), 1:200 (#07-330; Millipore); (10) partitioning defective 6 homolog (Par6), 1:200 (ab45394; Abcam); and (11) partitioning defective 1 homolog/microtubule affinity regulating kinase 2 (Par1/MARK2), 1:100 (sc-46607, Santa Cruz). Alexa Fluor phalloidin 555 (Molecular Probes), 25 μg/ml, was used to stain F-actin.

For whole-mount immunofluorescence, embryos were fixed in methanol (peripherin, XNIF), 80% ethanol (Arp2) or phosphate-buffered 10% formalin (all others) and processed as described (Dent et al., 1989) using fluorescent (TRITC, FITC) avidins. Cleared embryos (benzyl-alcohol:benzyl-benzoate, 1:2), were imaged on a Zeiss LSM 510 confocal microscope (10× Fluar, 0.5 NA; 20× Plan ApoChromat, 0.75 NA). Histochemistry of dissociated cell cultures was performed as described (Smith et al., 2006; Undamatla and Szaro, 2001); these were imaged with a Zeiss Apotome microscope (40× EC Plan Neofluar, Oil, 1.3 NA; 100× Plan Apo, Oil, 1.4 NA) equipped with a Zeiss Axiocam MRM REV2 camera. For double label immunofluorescence, Alexa Fluor 488 secondary antibodies and TRITC-avidin were used for successive fluorophores to minimize crossreactivity. Morphometry was performed from images using AxioVision 4 (Zeiss) software. Western blots of stage 29/30 were carried out as described (Liu et al., 2008).

Co-immunoprecipitation of hnRNP K-mRNP complexes was performed using 13 juvenile frog brains (Baroni et al., 2008; Liu et al., 2008) as described [Gene Expression Omnibus (GEO); accession GSE25207], using protein-G agarose (Sigma) coupled to hnRNP K antibody or *E. coli* β-galactosidase antibody (Z3783; Promega). Immunoprecipitated RNA quality was assessed on Bioanalyzer Pico Chips (Agilent Technologies), and the specificity of the reaction was confirmed by quantifying known hnRNP K-targeted RNAs by qRT-PCR (Applied Biosystems, ABI SDS 7900HT; ABI SDS software, version 2.2) using TaqMan One-Step RT-PCR Master Mix reagents (Applied Biosystems). Primer and probe sequences are listed in Table S1 in the supplementary material.

Microarray procedures
Co-immunoprecipitated RNAs were amplified, labeled (One Cycle Amplification, Affymetrix) and hybridized against *Xenopus laevis* 2.0 microarrays (Affymetrix) at the Center for Functional Genomics (University at Albany), using three arrays each for the specific and non-specific antibody samples. After raw data were corrected for background and filtered using MAS5 (Affymetrix), they were normalized across arrays [Proportional Variance – RMA (Bolstad et al., 2003)] and further filtered to remove the bottom 30th percentile (GeneSpring GX 10; Agilent).

Microarrays were validated by both conventional and quantitative RT-PCR (qRT-PCR). Co-immunoprecipitated RNAs were reverse-transcribed (oligo dT/SuperScript III, Invitrogen) and amplified by conventional (GoTaq Green, Promega) or quantitative (Power SYBR Green, Applied Biosystems) PCR; for primers, see Table S1 in the supplementary material. Conventional RT-PCR used both the same RNA as the microarrays and RNA freshly extracted from three brains. qRT-PCR was performed with fresh samples. Fold changes were determined using the $\Delta\Delta C_T$ method (Livak and Schmittgen, 2001) with 18S RNA as a loading control.

Microarray data have been deposited in GEO under accession number GSE25207.

Biochemical analyses
Developmental gene expression was assayed by qRT-PCR (SYBR Green) using total RNA (RNeasy Mini Kit, Qiagen) from 50 embryos each at stages 15, 20, 29/30 and 37/38, with *GAPDH* RNA as the loading control. Effects of hnRNP K-knockdown on expression of *Arp2*, *tau* and *XNIF* RNAs were assayed by qRT-PCR (SYBR Green) using total RNA of stage 29/30 embryos as above (three biological replicates per time point). Polysomal profiling and separation of nuclear from cytoplasmic RNAs (ten stage 29/30 embryos) were done as described (Ananthakrishnan et al., 2008; Liu et al., 2008), except that SYBR Green instead of TaqMan chemistry was used for qRT-PCR.

RESULTS
hnRNP K is essential for axon outgrowth during development
As demonstrated earlier (Liu et al., 2008), hnRNP K-knockdown by antisense MO led specifically to a nearly complete, cell-autonomous loss of axons in both intact embryos and dissociated cell culture (Fig. 1). This effect was due specifically to the loss of hnRNP K, as co-injection of in vitro transcribed hnRNP K RNA lacking the MO-targeting sequence largely restored axon outgrowth. Immunostaining for N-β tubulin and peripherin (Fig. 1Db and 1Cb, respectively), markers for terminally specified neurons, demonstrated that neurons were, nonetheless, present.

To gain further insights into the intracellular mechanism underlying this axonless phenotype, we stained neurons in dissociated embryonic neural tube/myotome cultures of bilaterally injected embryos for all three cytoskeletal polymers (Fig. 1Ea-Gc,Ic,Id) and for the cell polarity complex proteins Par6 (Fig. 1Ha-Ib) and Par3 (not shown, but indistinguishable from Par6), which function downstream of PI3-kinase/Akt/GSK-3β in specifying neuronal polarity (Yoshimura et al., 2006). In this culture system, neurites develop as axons; during the first two days, all eventually
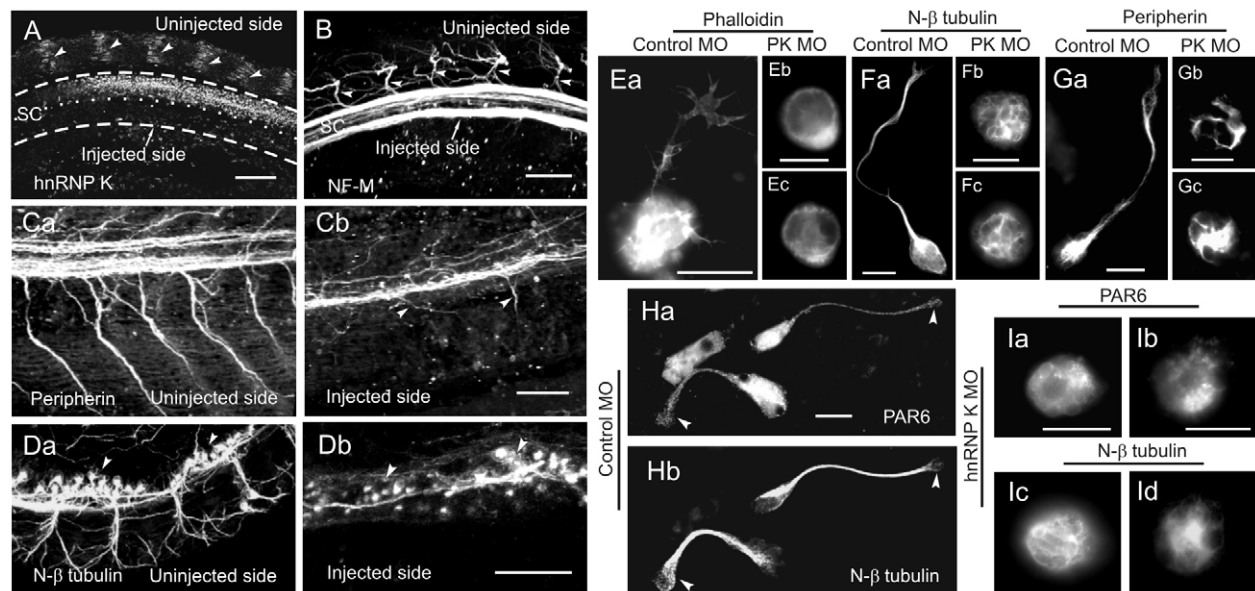
Fig. 1. Axon outgrowth and cytoskeletal organization, but neither neuronal specification nor early stages of cellular polarization, were severely compromised with hnRNP K knockdown. (**A**) Immunostained optical section of a stage 40 *Xenopus* tadpole demonstrates suppression of hnRNP K expression on the injected side by hnRNP K MO (below dots). SC (inside dashed lines), spinal cord; arrowheads, hnRNP K staining of muscle nuclei on the uninjected side. (**B-Db**) Suppression of axon outgrowth on the injected side of stage 40 tadpoles [B(bottom),Cb,Db] revealed by immunostaining for the indicated axonal markers. A and B are horizontal and Ca-Db parasagittal sections. Arrowheads in Cb and in Da and Db indicate examples of atrophied axons and neuronal perikarya, respectively. Arrowheads in B indicate normally projecting motor axons on the uninjected side. (**Ea-Gc**) Organization of the indicated cytoskeletal polymers was severely disrupted in neurons of bilaterally injected hnRNP K MO (PK MO) cultures compared with those of control MO (Ea,Fa,Ga), which appeared normal. With hnRNP K MO, F-actin circumscribed perikarya, but was asymmetrically distributed (Eb,Ec); microtubules formed an anastomosing network (Fb,Fc); neuronal intermediate filaments were twisted and radiated outward in multiple directions (Gb,Gc). (**Ha-Id**) Double immunostaining for N-β tubulin and Par6 as indicated. With control MO (Ha,Hb), Par 6 staining was punctate and filled neuronal perikarya and axons (arrowheads, growth cone). With hnRNP K MO (Ia-Id), neuronal perikaryal microtubules (Ic,Id) were poorly organized and failed to correspond with an asymmetric hotspot of Par6 immunostaining (Ia,Ib). Scale bars: 100 μm for A-Db; 20 μm for Ea-Id.

express axon-specific markers [e.g. phosphorylated NF-M (Lin and Szaro, 1994)] and many form fully functional synapses (Buchanan et al., 1989; Chow and Poo, 1985; Schaeffer et al., 1994). In control MO cultures, neuronal perikarya exhibited punctate Par3/6 immunostaining, which extended into nascent axons and the growth cone (Fig. 1Ha, arrowheads). The intracellular organization of cytoskeletal polymers of control MO cultured neurons was also normal (Fig. 1Ea,Fa,Ga,Hb). In bilaterally injected hnRNP K MO cultures, Par3/6 perikaryal immunostaining in neurons (i.e. N-β tubulin-positive cells) was markedly asymmetrical (Fig. 1Ia,b). Although no filopodia or F-actin-labeled focal contacts were evident, the F-actin circumscribing the perikaryal periphery accumulated preferentially to one side (Fig. 1Eb,c). This asymmetry of Par3/Par6 and F-actin indicated that cells had progressed through at least the early stages of polarization, but this polarization did not extend to the reorganization of microtubules (N-β tubulin) and neuronal intermediate filaments (peripherin) that is characteristic of neurons with axons. Instead, microtubules formed an anastomosing network, out of register with the hotspot of Par3/Par6 staining (Fig. 1Ia-d), and peripherin formed multiple, twisted filaments radiating outward from the nucleus (Fig. 1Gb,c). Thus, loss of hnRNP K severely disrupted cytoskeletal polymer organization downstream of neuronal specification, of the initial events leading to neuronal polarity and of cytoskeletal polymer synthesis but upstream of reorganizing these polymers to form an axon.

Prospective hnRNP K mRNA targets were identified by RNA-binding protein immunoprecipitation microarray (RIP-Chip)

To identify targets of hnRNP K, we used RIP-chip (Fig. 2A,B) of juvenile froglet brain to obtain exclusively neural transcripts from mature as well as developing neurons, because *Xenopus* juvenile brain undergoes considerable neuro- and axonogenesis (Grant and Keating, 1986) and contains a substantial population of neurons expressing Par1, Par3 and Par6 (see Fig. S1 in the supplementary material). To assay the suitability of juvenile brain for this analysis, we quantified co-immunoprecipitated *NF-M* and *GAP43* RNAs, which are known hnRNP K targets, and *peripherin* and 18S rRNA, which are known not to be (Irwin et al., 1997; Liu et al., 2008; Thyagarajan and Szaro, 2004); upregulated *GAP43* expression is a hallmark feature of neurons with actively growing axons (Benowitz et al., 1981; Skene and Willard, 1981). As predicted, the two hnRNP K target-RNAs were significantly abundant in the hnRNP K immunoprecipitate compared with that of β-galactosidase, whereas the two non-target RNAs were not (Fig. 2C).

A cutoff of fourfold enrichment between specific and non-specific antibody arrays was used to select candidate target-transcripts. This cutoff was chosen because a statistical comparison of enrichment between hnRNP K and β-galactosidase arrays in both directions predicted it would limit false positives to ~1-2%, and because it successfully captured all three known neural hnRNP K-associated transcripts [i.e. *GAP-43*, *NF-L* and *NF-M* (Irwin et
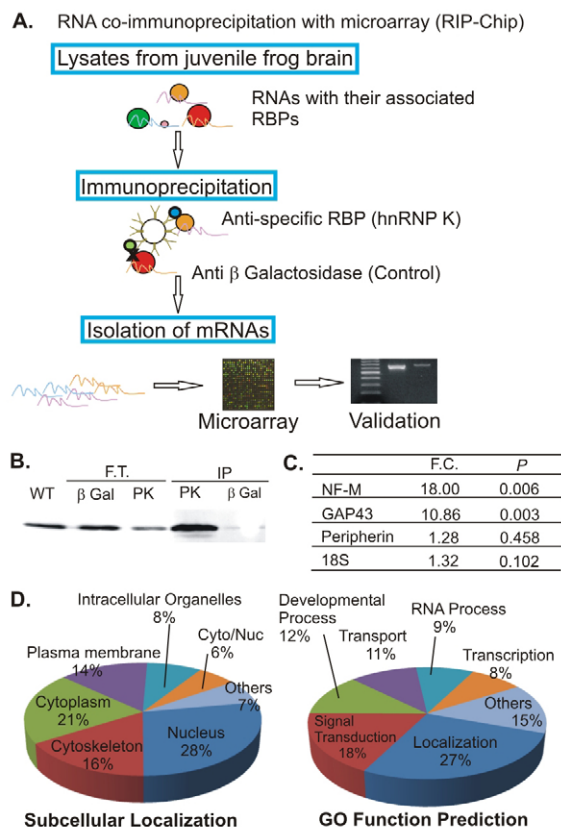
Fig. 2. Endogenous hnRNP K RNA targets, identified by RIP-chip from juvenile brain, are enriched for cytoskeletal transcripts and those involved in intracellular localization and transport.
(**A**) Schematic of the RIP-chip strategy. RBP, RNA-binding protein.
(**B**) Chemiluminescent western blot demonstrates that hnRNP K was enriched by immunoprecipitation with anti-hnRNP K (PK) but not by anti-β-galactosidase (βGal) in the immunoprecipitate (IP) relative to the flow through (F.T.). (**C**) Fold changes (F.C.) for indicated transcripts in hnRNP K versus β-galactosidase co-immunoprecipitations, assayed by qRT-PCR (TaqMan). *P*, significance by *t*-test (three biological replicates each). (**D**) Classification of annotated genes from the arrays by DAVID according to Gene Ontology (GO) terms for subcellular localization and biological function (*P*<0.05).

Fig. 3. Validated transcripts increase in expression with axon outgrowth. (**A**) Validation by conventional RT-PCR. PK and βGal RT-PCR products from hnRNP K and β-galactosidase co-immunoprecipitations, respectively, visualized on ethidium bromide-stained agarose gels. Only *profilin2* (PFN2) failed to amplify from hnRNP K co-immunoprecipitated RNA. (**B**) Developmental expression analysis of a subset of validated transcripts by qRT-PCR (SYBR Green). All but NF-L (NEFL) robustly increased expression between stages 20 (axon initiation) and 29/30 (the peak period of axon outgrowth). Values are plotted relative to expression at stage 37/38. Error bars, s.d.(three biological replicates). See Table S1 in the supplementary material for definitions of gene symbols.

al., 1997; Thyagarajan and Szaro, 2004; Thyagarajan and Szaro, 2008)]. The final list contained 753 transcripts, which included 130 genes that are fully annotated in *Xenopus* (see Table S2 in the supplementary material) plus 623 hypothetical proteins and expressed sequence tags (ESTs). Although we concentrated on the fully annotated genes, the entire set of microarray data is publicly available [NIH GEO database; GSE25207]. The annotated genes were then analyzed by DAVID [Database for Annotation, Visualization and Integrated Discovery (Huang et al., 2009)] to classify them by subcellular localization (Fig. 2D, left) and intracellular biological function (Fig. 2D, right). Consistent with effects of hnRNP K-knockdown on the cytoskeleton, a substantial portion of transcripts represented cytoskeletal-associated proteins (16%; *P*<0.001), although nuclear proteins were also highly represented (28%). The largest functional groups were transport (11%) and localization (27%), which included many cytoskeletal-associated transcripts.
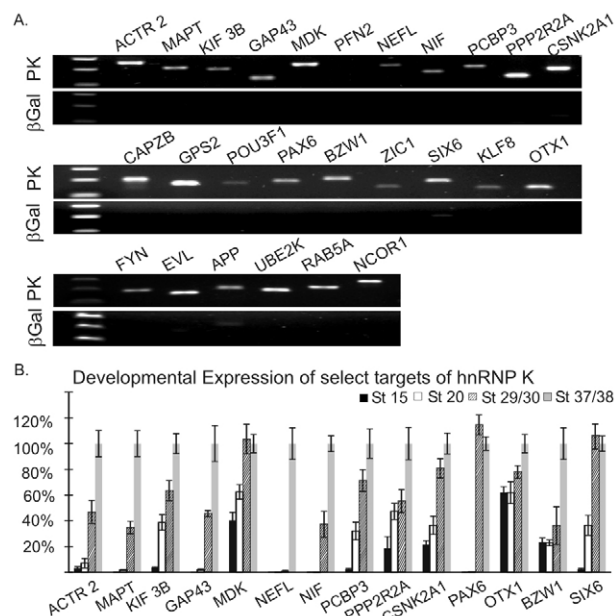
Validation of and developmental expression of RIP-Chip-identified hnRNP K-associated RNAs

Twenty-seven transcripts were selected for validation by conventional (Fig. 3A) and qRT-PCR (Table 1; *P*<0.02, *t*-test of three independent samples) because of their associations with the cytoskeleton, growth and maintenance of axons, or neural development in general. All except *profilin2* were successfully validated. Reasoning that transcripts involved in axon outgrowth should increase in expression with the onset of axon outgrowth, we next analyzed by qRT-PCR the expression of fourteen of these at key developmental stages (Fig. 3B): stages 15 (neural fold, the onset of neuronal differentiation), 20 (neural tube, the onset of axon outgrowth), 29/30 (tailbud, the peak of axon outgrowth) and 37/38 (2-day-old, newly hatched tadpole). All except *NF-L*, which is known to increase after axons contact targets (Undamatla and Szaro, 2001), increased with the onset of axon outgrowth between stages 20 and 29/30 (average fold increase, 314; *P*<0.05, $t_{3,3}$-test).

Consensus sequences for RNA binding to hnRNP K were present in most validated transcripts

We next examined transcripts for the presence of two known hnRNP K RNA-binding consensus sequences: one determined by SELEX [systematic evolution of ligands by exponential enrichment; 5′-UC$_{3-4}$(U/A)(A/U)-3′ (Thisted et al., 2001)], and another identified by bioinformatics and confirmed by direct binding experiments [CCAUCN$_{2-7}$(A/U)CCC(A/U)N$_{7-18}$UC-

A(C/U)C (Klimek-Tomczak et al., 2004)]. Whereas the first is predicted to interact with just a single KH domain, the second, longer, tripartite sequence is predicted to interact with all three KH domains of hnRNP K, which confers stronger binding to RNAs (Paziewska et al., 2004; Thisted et al., 2001). Twenty-four (92%)

of the validated transcripts contained at least one copy of the shorter, SELEX-identified sequence (Table 1), and seventeen (65%) contained the longer tripartite motif (Fig. 4), which was located preferentially (13/17) within 3′-UTRs. Consistent with additional requirements for hnRNP K-binding (Thisted et al.,

Table 1. Validation of select hnRNP K-associated transcripts by quantitative RT-PCR

Symbol	Gene name	*Xenopus* UniGene	Human UniGene	Array F.C.*	qRT-PCR F.C.[†]	*P*	Function	Number of SELEX sequences[§]
ACTR2	Actin Related Protein 2	Xl.22948	Hs.643727	25.7	44.6	0.001	Actin branching / Filopodia formation	2
PFN2	Profilin 2	Xl.77241	Hs.91747	14.8	N/A	N/A	Actin polymerization / Axon guidance	N/A
EVL	Enah/Vasp-like	Xl.63457	Hs.125867	5.8	8.3	0.013	Actin filament organization / Axon guidance	2
MAPT	Microtubule-Associated Protein Tau	Xl.2716	Hs.101174	12.6	28.7	0.002	Microtubule bundling, stabilization / Alzheimer's disease	5
KIF3B	Kinesin Family Member 3B	Xl.1113	Hs.369670	24.4	34.0	0.010	Axonal transport / Neuronal polarization	6
NEFM	Neurofilament, middle polypeptide (NF-M)	Xl.173	Hs.723845	8.21	18.0[‡]	0.006	Axon cytoskeleton / ALS	2
NEFL	Neurofilament, light polypeptide (NF-L)	Xl.991	Hs.521461	4.7	9.7	0.005	Axon cytoskeleton / ALS	3
NIF	Low molecular weight Neurofilament (XNIF)	Xl.992	Hs.500916	4.9	32.9	0.015	Axon cytoskeleton	4
PPP2R2A	Protein phosphatase 2A	Xl.734	Hs.146339	4.2	14.5	0.035	Dephosphorylation of neurofilaments	0
CSNK2A1	Casein Kinase 2, alpha 1 polypeptide	Xl.11560	Hs.644056	6.8	11.6	0.001	Phosphorylation of neurofilaments	3
GAP43	Growth Associated Protein 43 a	Xl.1133	Hs.134974	5.3	16.2	0.004	Axonal outgrowth (development/ regeneration)	1
MDK[¶]	Midkine (pleiotrophic factor-alpha2)	Xl.899	Hs.82045	9.0	14.8	0.002	Neurite growth promoting factor	4
FYN	FYN oncogene related to SRC, FGR, YES	Xl.21919	Hs.390567	6.9	15.1	0.011	Tyrosine-protein kinase / Axon guidance	4
RAB5A	RAB5A, member RAS oncogene family	Xl.2484	Hs.475663	17.3	23.0	0.001	Neurite outgrowth and branching / ALS	2
APP	Amyloid beta (A4) precursor protein	Xl.83164	Hs.434980	15.1	30.2	0.001	Alzheimer's disease	8
UBE2K	Ubiquitin-conjugating enzyme E2K	Xl.6363	Hs.50308	6.32	21.8	<0.001	Huntington's disease	1
NCOR1	Nuclear receptor co-repressor 1	Xl.77498	Hs.462323	7.21	10.9	0.001	Huntington's disease	11
PAX6	Paired box 6	Xl.647	Hs.270303	11.3	16.3	0.009	Eye development	3
BZW1	Basic leucine zipper and W2 domains 1	Xl.76633	Hs.355983	9.3	22.5	0.001	Eye development	2
OTX1	Orthodenticle homeobox 1	Xl.781	Hs.445340	9.0	17.7	<0.001	Brain and sensory organ development	2
ZIC1	Zic family member 1 (odd-paired homolog)	Xl.1796	Hs.647962	6.1	12.9	0.001	Neural determination and patterning	5
POU3F1	POU class 3 homeobox 1	Xl.21449	Hs.1837	5.6	9.5	0.001	Brain development	2
SIX6	SIX homeobox 6	Xl.533	Hs.194756	4.2	8.5	0.001	Eye development	1
KLF8	Kruppel-like factor 8	Xl.17318	Hs.646614	5.8	21.4	<0.001	Vertebrate development	4
PCBP3[¶]	Poly(rC) binding protein 3 (hnRNP E2)	Xl.70063	Hs.546271	7.6	22.7	0.007	RNA-binding protein / Neural development	7
CAPZB[¶]	Capping protein muscle Z-line, beta	Xl.76987	Hs.432760	12.8	19.4	<0.001	Actin Capping / Growth of actin filament	0
GPS2[¶]	G protein pathway suppressor 2	Xl.34962	Hs.438219	18.0	34.5	0.001	JNK signaling pathway	2

F.C., fold change; N/A, not applicable.
*F.C. on the microarrays was calculated by the GeneSpring GX10 program.
[†]F.C. was calculated by quantitative RT-PCR (SYBR Green, except for [‡], which was obtained from TaqMan); *P* value was obtained by Student's *t*-test performed on qRT-PCR data.
[§]The coding and 3′ UTR sequences of target mRNAs were screened for the number of SELEX-predicted binding motifs they contained: 5′-UC$_{3-4}$(U/A)$_2$-3′ (Thisted et al., 2001).
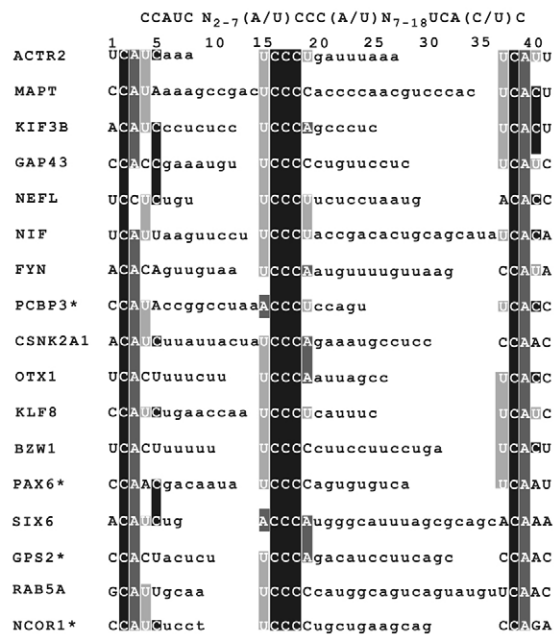[¶]These target mRNAs associate with hnRNP E2 in a hematopoietic cell line (Waggoner and Liebhaber, 2003).

```
                     CCAUC N2-7 (A/U) CCC (A/U) N7-18 UCA (C/U) C
             1    5    10   15   20   25   30   35   40
ACTR2     UCAUCaaa          UCCCUgauuuaaa               UCAUU
MAPT      CCAUAaaaagccgacUCCCCaccccaacgucccac           UCACU
KIF3B     ACAUCccucucc   UCCCAgcccuc                    UCACU
GAP43     CCACCgaaaugu   UCCCCcuguuccuc                 UCAUC
NEFL      UCCCUcugu      UCCCUucuccuaaug                ACACC
NIF       UCAUUaaguuccu  UCCCUaccgacacugcagcaua         UCACA
FYN       ACACAguuguaa   UCCCAauguuuuguuaag             CCAUA
PCBP3*    CCAUAccggccuaaACCCUccagu                      UCACC
CSNK2A1   ACAUCuuauuacuaUCCCAgaaaugccucc                CCAAC
OTX1      UCACUuuucuu    UCCCAauuagcc                   UCACC
KLF8      CCAUCugaaccaa  UCCCUcauuuc                    UCAUC
BZW1      UCACUuuuuu     UCCCCcuuccuuccuga              UCACU
PAX6*     CCAACgacaaua   UCCCAcaguguguca                UCAAU
SIX6      ACAUCug      ACCCAugggcauuuagcgcagcACAAA
GPS2*     CCACUacucu     UCCCAgacauccuucagc             CCAAC
RAB5A     GCAUUgcaa      UCCCCcauggcagucaguauguUCAAC
NCOR1*    CCAUCucct      UCCCCugcugaagcag               CCAGA
```

Fig. 4. An hnRNP K tripartite RNA-binding consensus sequence (top) was present in a majority of the validated targets. Shading indicates nucleotides matching core nucleotides (i.e. those necessary for binding) in at least 50% of the cases. Asterisks indicate transcripts in which the motif is found in the coding region; all others are in the 3′-UTR.

2001), M-fold plots (Zuker, 2003) predicted that the central 'CCC' lay within a single stranded region of a hairpin-loop in ten of the 17, including *tau* (not shown).

Injection of synthetic RNA containing multiple copies of the tripartite binding motif into embryos phenocopied hnRNP K-knockdown

To further test the hypothesis that hnRNP K affects axonogenesis through pleiotropic effects on targeted RNAs, we constructed a synthetic, non-coding RNA containing either one or three tandem repeats of the tripartite binding motif (single or triple tripartite binding motif, respectively) of *tau* (see Table S1 in the supplementary material). Control RNAs contained three copies of either (1) a tripartite motif wherein nucleotides required for hnRNP K-binding were mutated by transversions (triple mutated-tripartite motif), or (2) a randomly scrambled version of the entire motif (triple scrambled-tripartite motif). Motifs were spliced upstream of the 3′-UTR of rabbit β-*globin* to stabilize the RNAs in embryos (Vize et al., 1991) and to mimic the in vivo scenario in which the RNA-binding sequence is embedded within a longer 3′-UTR. The motifs themselves contained neither a start codon nor an open reading frame (ORF), although a short (~100 nucleotide) ORF was located downstream, within the β-*globin* sequences and was, therefore, present in all three RNAs. The rationale was that introducing into *Xenopus* embryos a synthetic RNA bearing multiple copies of the stronger binding motif should mimic effects of hnRNP K knockdown by acting as a molecular sponge to competitively inhibit the normal activity of hnRNP K within the cytoplasm (Tripathi et al., 2010).

RNAs were injected into 2-cell embryos, and the subsequent effects on nervous system development in vivo were analyzed by whole-mount immunostaining at stage 37/38 for three neuronal

antigens: NF-M, RNA for which was a target of hnRNP K, and peripherin and N-β tubulin, RNAs for which were not. With the triple binding-motif RNA, the intensity of NF-M immunostaining, which is also suppressed with hnRNP K knockdown (Liu et al., 2008), was reduced (Fig. 5Ab) and outgrowth of peripheral motor and sensory axons was severely compromised (Fig. 5Ab-d). As with hnRNP K-knockdown, positive staining of perikarya for N-β tubulin (Fig. 5Ac) indicated that neuronal specification was unperturbed and that axon outgrowth, as opposed to immunostaining, was affected directly. Control RNAs yielded overt defects in neither axon outgrowth nor NF-M expression (Fig. 5Ba,Ca versus 5Bb,Cb).

To confirm that effects were cell autonomous, we examined neurons (N-β tubulin-positive) in cell cultures of dissociated embryonic spinal cord/myotomes. With the triple tripartite binding-motif RNA, but not controls, a substantial portion of neurons either lacked neurites entirely or developed only short, immature ones, and the organization of their microtubules was severely disrupted (Fig. 5Da-d). Three quantitative measures confirmed effects on axon outgrowth: (1) the percentage of N-β tubulin-positive cells possessing one or more neurites (Fig. 5E, top), (2) total neurite length (Fig. 5E, bottom left), and (3) branching of the primary neurite (Fig. 5E, lower right). Relative to uninjected controls, all three measures were significantly reduced ($P<0.01$; t-test, four and three pairs of cultures for measures 1 and 2-3, respectively) in cultures made from embryos unilaterally injected with the triple tripartite binding-motif RNA, but not in those of control RNAs. Moreover, effects on neurite outgrowth with the RNA bearing only the single tripartite binding-motif were intermediate between controls and the triple tripartite motif (Fig. 5E), which further supported the argument that effects on axonogenesis were caused by competitive inhibition of the binding of hnRNP K to its native targets.

Cytoskeletal-associated transcripts belong to the same hnRNP K-associated RNA regulon

RNA regulons (or operons) coordinate the fates of functionally interrelated mRNAs within a cell through the actions of shared RNPs binding to similar sequence elements (Keene, 2007; Keene and Tenenbaum, 2002). Any single RNP, such as hnRNP K, can, nonetheless, participate in multiple regulons, depending on the context (Bomsztyk et al., 2004). To test whether cytoskeletal-associated transcripts comprise an hnRNP K-dependent RNA regulon governing neuronal cytoskeletal-associated proteins needed for axon outgrowth, we selected three validated transcripts, which mediate polymer interactions and expression of which increased with the onset of axon outgrowth: *Arp2* (gene symbol ACTR 2), *tau* (gene symbol MAPT), and *XNIF* (gene symbol NIF). We predicted that transcripts belonging to the same regulon would be regulated similarly by hnRNP K.

To test this prediction, we first verified that hnRNP K regulated all three transcripts post-transcriptionally. Whereas hnRNP K MO embryos at stage 29/30 expressed comparable levels of *Arp2*, *tau* and *XNIF* RNAs as controls (Fig. 6A; $P>0.1$, one-way ANOVA), they expressed much less protein, as determined both by western blot (Fig. 6B) and whole-mount immunohistochemistry (Fig. 6Ca,b,Da,b,Ea,b). Co-injection of in vitro transcribed *Xenopus hnRNP K* RNA lacking the MO targeting site effectively restored protein expression (Fig. 6Cc,Dc,Ec), confirming that effects were specific to hnRNP K-knockdown and were not off-target effects.
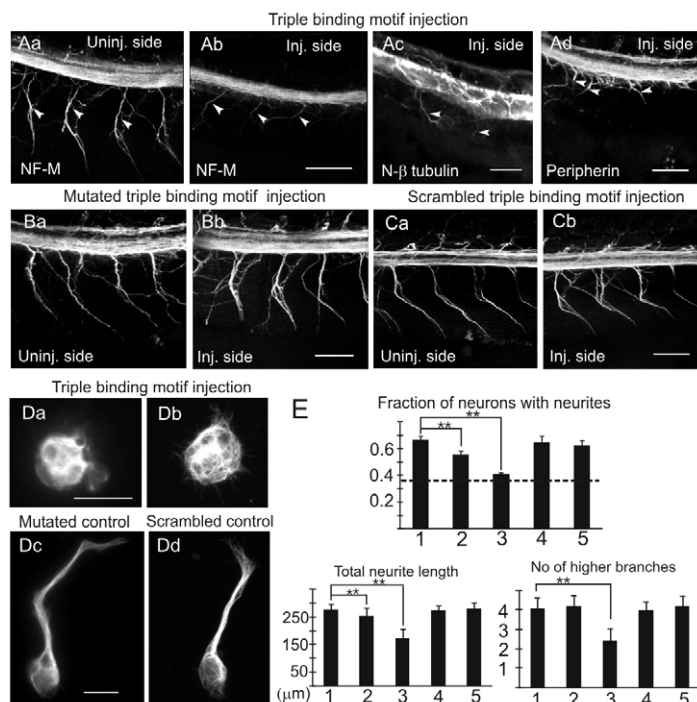
Fig. 5. Axon outgrowth was suppressed by injection into embryos of a non-coding RNA bearing the triple tripartite hnRNP K RNA-binding motif. (**Aa-Cb**) Parasagittal optical sections of whole-mount immunostained stage 37/38 animals. (Aa-Ad) Animals receiving the triple tripartite binding motif. Aa shows the uninjected (Uninj.) side with arrowheads indicating motor axons. Animals were immunostained for the indicated axonal markers (NF-M; peripherin; neuronal (N) β-tubulin). Arrowheads in Ab-Ad point to severely atrophied fibers. (Ba-Cb) Two control RNAs yielded normal axon outgrowth and expression of NF-M on the injected side. Scale bars: 100 μm. (**Da-Dd**) In dissociated embryonic spinal cord cultures, the triple tripartite binding motif RNA yielded neurons (positively stained for N-β tubulin) with marked defects in microtubule organization and that either lacked neurites (Da) or had only short, immature neurites (Db). Neurons from indicated control RNA cultures (Dc,Dd) were normal. Scale bars: 20 μm. (**E**) Top: Mean (± s.d.) fraction of N-β tubulin-positive cells that had neurites. Bottom left: Mean (± s.d.) total length of neuritic arbor per cell. Bottom right: Mean (± s.d.) number of higher order branches (secondary and higher) per cell. 1, uninjected; 2, single tripartite binding motif-injected; 3, triple tripartite binding motif-injected; 4, triple mutated tripartite motif-injected; 5, triple scrambled tripartite motif-injected cultures. Because embryos were unilaterally injected, only the half derived from the uninjected side was expected to be normal (indicated by dashed line). **$P<0.01$, t-test. Numbers of neurons tabulated were: upper graph (four cultures each), bars 1-5: 610, 625, 631, 591, 632, respectively; lower graphs (three cultures each), bars 1-5: 169, 158, 155, 142, 184, respectively.

To identify how hnRNP K regulated these transcripts, we assayed mRNA nuclear export and loading onto polysomes, as carried out previously for *NF-M* (Liu et al., 2008). qRT-PCR of nuclear and cytoplasmic fractions indicated that the cytoplasmic/nuclear ratio ($\Delta\Delta C_T$ between nuclear versus cytosolic fractions) was significantly less for *Arp2*, *tau* and *XNIF* RNAs of bilaterally injected, hnRNP K MO embryos compared with control MO [22-, 34-, 37-fold ($\sim2^{\Delta\Delta C_T}$) reductions, respectively; $P<0.01$, $t_{3,3}$-test]; these defects were comparable to that seen for *NF-M* ($\sim$31-fold) (Fig. 7A). No such defect was seen for the non-targeted RNA *peripherin*, confirming it was not a generalized defect in RNA nuclear export. Polysomal profiling demonstrated a direct effect on translation. For example, *Arp2* RNA of stage 29/30 embryos bilaterally injected with hnRNP K MO was less abundant in the heavier, efficiently translated polysomal fractions (Fig. 7B; P) than was the case with control MO. For all three cytoskeletal-associated transcripts, the percentage of RNA present in polysomal fractions [Fig. 7C; average of three biological replicates ± s.e.m., ten embryos each] was significantly reduced for hnRNP K MO- versus control MO-injected animals (*Arp2*, 14 versus 52%; *tau*, 18 versus 44%; *XNIF*, 19 versus 33%, respectively; $P<0.01$, t-test). This was not the case for *peripherin*, indicating that the defect was not a generalized defect on RNA translation.

To test whether hnRNP K regulated all targeted transcripts in the same manner, polysomal profiling was done for three additional RNAs: two nuclear transcripts (*Otx1*, *Pax6*) and a non-cytoskeletal-associated transcript involved in membrane trafficking from the Golgi (*Rab5a*) (see Fig. S2 in the supplementary material). Whereas *Rab5a* exhibited a shift from polysomal fractions (47 to 27% between hnRNP K and control MO), *Otx1* (39 to 42%) and *Pax6* (34 to 39%) did not, suggesting that *Rab5a* belongs to the same and the other two belong to different hnRNP K-associated RNA regulons than the four cytoskeletal-associated transcripts.

Simultaneous knockdown of multiple, but not individual, hnRNP K-targeted cytoskeletal-associated RNAs compromised axon outgrowth

To determine the degree to which the loss of cytoskeletal-associated proteins caused by hnRNP K-knockdown contributed to defects seen in cytoskeletal polymer organization and axon outgrowth, we targeted Arp2, tau and XNIF expressions directly using antisense MOs. We reasoned that if the hnRNP K-knockdown defects in cytoskeletal polymer organization, and therefore axon outgrowth, involved pleiotropic effects on this group of transcripts, then defects caused by directly knocking down all three simultaneously should be greater than those caused by targeting each one individually. All three MOs successfully suppressed expression of their respective targets (see Fig. S3 in the supplementary material) and, by all external criteria, injected tadpoles were overtly normal, indicating that there were no off-target effects on overall development. Whole-mount immunostaining at stage 37/38 for peripherin revealed relatively mild, individualized effects on peripheral motor and sensory axons with Arp2 and tau single-MO injection (Fig. 8Ab,Bb), consistent with their known functions. Peripheral nerves formed and projected successfully to the same target areas on the injected side as on the uninjected side, although they appeared less robust than normal (Fig. 8Aa-Bb). Because earlier studies had already shown that depleting *Xenopus* neurons of XNIF and NF-M slows axon elongation without interfering with either the formation and targeting of axons or the axonal transport of actin and tubulin, we did not repeat the knockdown of XNIF individually (Lin and Szaro, 1995; Lin and Szaro, 1996; Szaro et al., 1991; Walker et al., 2001). Thus, effects on axon outgrowth from suppressing expression of each transcript individually were milder than those seen with hnRNP K-knockdown. However, when all three cytoskeletal-associated MOs were co-injected, effects were synergistically magnified, with peripheral nerve outgrowth being severely compromised (Fig. 8Ca,Cb), yielding a close, although not identical, phenocopy of hnRNP K-knockdown.
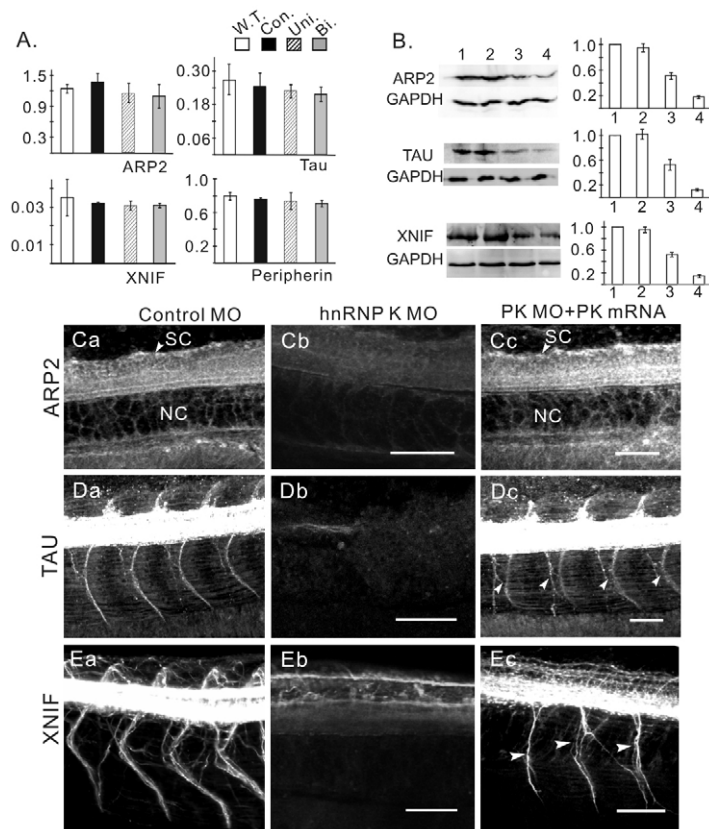
Fig. 6. hnRNP K MO inhibits protein but not mRNA expression of select targets in vivo. (**A**) qRT-PCR (SYBR Green) for identified hnRNP K cytoskeletal target (*Arp2*, *tau*, *XNIF*) and non-target (*peripherin*) RNAs. Ordinate, fold difference relative to loading control (*GAPDH* RNA). Differences were insignificant among the groups (one-way ANOVA, $P>0.1$). W.T., uninjected wild type; Con., control MO-injected; Uni. or Bi., unilaterally or bilaterally injected, respectively, with hnRNP K MO. (**B**) Chemiluminescent western blot and quantified band intensities for Arp2, tau and XNIF (after normalization to GAPDH) relative to uninjected controls. (1) uninjected controls; (2) unilaterally injected, control MO: 95±6%; 102±8%; 96±5%, respectively; (3) unilaterally injected, hnRNP K MO: 54±6%, 53±9%, 52±4%, respectively; (4) bilaterally injected, hnRNP K MO: 18±3%, 12±2%, 15±3%, respectively. (**Ca-Ec**) Parasagittal, confocal, optical sections of stage 29/30 embryos injected with MO and immunostained for Arp2 (Ca-Cc), tau (Da-Dc), and XNIF (Ea-Ec). Normal expression is seen with control MO (Ca,Da,Ea) but was effectively suppressed by hnRNP K MO (Cb,Db,Eb). Inhibition of Arp2, XNIF and tau expression was effectively restored by co-injection of hnRNP K RNA with the antisense MO (Cc,Dc,Ec). Note that axon outgrowth was also rescued, as seen with tau and XNIF (Dc,Ec, arrowheads). Optical sections for Arp2 are too close to the midline to view axons (Ca-Cc). SC, spinal cord. Ca-Cc contain notochord (NC), whereas Da-Ec contain motor axons and somites. Rostral is left in Da-Dc and right in Ca-Cc,Ea-Ec. Scale bars: 100 µm.

To confirm that effects were cell-autonomous, we examined them in more detail in dissociated cell cultures of bilaterally injected embryos. Knockdown of Arp2 by itself had little effect on neurite outgrowth per se: neurites formed as often (Fig. 8Da-d) and elongated as much as in controls (Fig. 8De). Nonetheless, phalloidin staining for F-actin revealed abnormal growth cone morphologies with the Arp2 MO compared with control MO (Fig. 8Da-d). Also, Arp2-knockdown yielded neurites with ~15% fewer branches than controls (Fig. 8De; $P<0.01$, *t*-test, three cultures), but no other quantitatively significant defects. With knockdown of tau by itself, cultured neurons appeared even more morphologically normal than with Arp2 knockdown, and neither neurite elongation nor branching was altered significantly (Fig. 8Ee), consistent with findings from tau-knockout and tau-depleted neurons cultured from rodents (Harada et al., 1994; Tint et al., 1998). Tau knockdown nonetheless deleteriously affected microtubule architecture (Fig. 8Eb,Ed), consistent with its known role in promoting microtubule elongation and alignment (Cleveland et al., 1977). Thus, suppressing the expression of each of the cytoskeletal-associated proteins individually led to different defects, indicating that their functions were not redundant; moreover, each led to only relatively mild defects in axongenesis.

In sharp contrast, neurite outgrowth was dramatically compromised by co-injection of all three MOs (Fig. 8Fa-e). Neurite extension and branching were significantly reduced (Fig. 8Fe; $P<0.01$, *t*-test), with many cells forming no neurites at all, compared with those receiving an equivalent quantity of control MO. Although filopodia still formed, which was not the case with hnRNP K-knockdown, F-actin staining was heavily circumscribed around the perikaryal periphery, yet asymmetrically distributed (Fig. 8Fb), closely reminiscent of what happened with hnRNP K-

knockdown. Also, microtubules were severely disorganized and mainly restricted to perikarya (Fig. 8Fd). Thus, the concomitant suppression of selected hnRNP K-regulated cytoskeletal-associated transcripts was synergistic, yielding in both the intact animal and dissociated cell culture a neuronal phenotype that approximated the severe defects associated with hnRNP K-knockdown.

DISCUSSION
Our study builds on foundations of an earlier study that demonstrated that hnRNP K is essential for axon outgrowth and investigated how hnRNP K post-transcriptionally regulates *NF-M* RNA, a validated target (Liu et al., 2008). The current study significantly extends our understanding of the post-transcriptional regulation by hnRNP K of genes involved in axon outgrowth by demonstrating that it regulates multiple transcripts associated not only with NFs but also with microtubules and microfilaments. The strong similarities of defects caused by simultaneously and directly knocking down expression of hnRNP K-targeted transcripts associated with all three cytoskeletal polymers to those caused by hnRNP K-knockdown indicates that pleiotropic effects on cytoskeletal-associated targets are a chief contributor to the axonless phenotype.

More importantly, this study provides the first direct experimental evidence that hnRNP K is the nexus of a novel, post-transcriptional regulatory module that coordinates the synthesis of structural proteins used to organize microtubules, microfilaments and NFs into an axon. Although traditionally studied individually, these polymers in fact participate in a tensegrity structure (Ingber, 2003), forming a network for which structuromechanical properties depend on interactions among the various polymer types, which are mediated by proteins that associate with each polymer. For

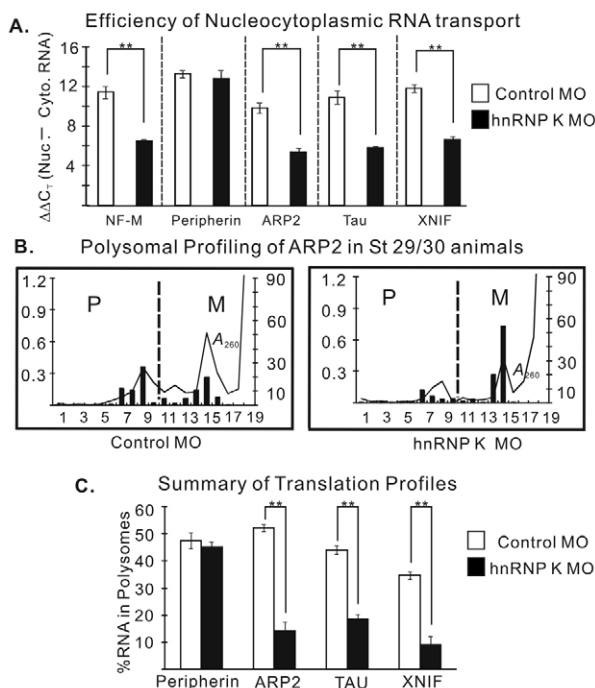**Fig. 7. hnRNP K MO yields defects in nuclear export and translation of *Arp2*, *tau* and *XNIF*, but not *peripherin*, RNAs.**
(**A**) qRT-PCR (SYBR Green) of nuclear and cytosolic fractions of stage 29/30, bilaterally injected embryos. $\Delta\Delta C_T$: mean ($\pm$ s.d.) difference in the number of PCR cycles to reach threshold. **$P<0.01$, t-test on three biological replicates. (**B**) Polysome profile of *Arp2* RNA at stage 29/30 indicates a shift from polysomal fractions (P) toward monosomal and premonosomal fractions (M) with hnRNP K-knockdown. Abscissa, fraction number. Solid line, total RNA (A_{260}), left ordinate. Bars, fraction of *Arp2* RNA present in each fraction, expressed as a percentage of total *Arp2* RNA present in the gradient, right ordinate. (**C**) The percentage of each RNA present in polysomal fractions for *Arp2*, *tau*, *XNIF* and *peripherin* mRNAs ($\pm$ s.e.m.). hnRNP K MO embryos exhibited significantly less (**$P<0.01$, t-test) *Arp2*, *tau* and *XNIF* RNA (hnRNP K targets) in polysomal fractions; *peripherin* RNA (not an hnRNP K target) exhibited no significant change.

example, Type IV neuronal intermediate filaments (e.g. NF-L, NF-M and α-internexin-like subunits) possess extensive carboxy-terminal domains that radiate outward from the filament and interact with both adjacent NFs and microtubules to preserve their alignment (Geisler et al., 1983; Hirokawa et al., 1984; Miyasaka et al., 1993). Similarly, tau not only aligns axonal microtubules but also mediates microtubule-microfilament interactions (Farias et al., 2002; Hirokawa et al., 1988; Weingarten et al., 1975), and Arp2, as part of the Arp2/3 complex, both forms branch points of the microfilament network and bridges them to microtubules through WHAMM [WAS protein homolog associated with actin, golgi membranes and microtubules (Campellone et al., 2008; Disanza and Scita, 2008)].

The results of the single- and triple-knockdown experiments for XNIF, Arp2 and tau demonstrated this tensegrity principal at work. The defects seen with individually disrupting expression of each cytoskeletal-associated protein were consistent with their known roles in consolidating axon outgrowth, organizing microtubules into parallel arrays, and filopodia-formation and filament-branching, respectively, none of which compromised the overall

length and patterning of axon outgrowth severely. By contrast, triple knockdown of these proteins led synergistically to severe defects in axon outgrowth accompanied by an uncoupling of the cytoskeletal polymers, which were, nonetheless, synthesized. Although a nice demonstration of tensegrity at work, more fundamental is the novel finding that the expressions of proteins fulfilling this tensegrity function are post-transcriptionally co-regulated through a shared RNA-binding protein.

The close partnership between transcriptional and post-transcriptional control of gene expression is a theme of growing importance for development, where it is used to fine-tune protein expression by directing it to where it is needed within the cell and by coupling it more directly with local signaling cascades. Examples of this partnership for the cytoskeleton include control of translation and nuclear export of actin mRNA in growth cones and sea urchin embryonic ectoderm, respectively (Gagnon et al., 1992; Leung et al., 2006; Yao et al., 2006), and the temporal and spatial refinement of N-β tubulin transcription in *Xenopus* animal cap cells culminating in neuron-specific expression of the protein (Oschwald et al., 1991). A similar partnership exists for Type IV NFs in the developing mammalian nervous system (Moskowitz and Oblinger, 1995; Schwartz et al., 1990; Schwartz et al., 1992), and its direct coupling to axon outgrowth is made clear in studies of regenerating *Xenopus* optic axons. Whereas unilateral nerve crush triggers rapid increases in *NF-M* and *XNIF* transcription in injured and uninjured eyes alike, only in the injured eye does this increase result in increased levels of expression and translation of cytoplasmic NF mRNAs (Ananthakrishnan et al., 2008; Ananthakrishnan and Szaro, 2009). Localization of transcripts belonging to multiple functional groups to growth cones and the leading edge of fibroblasts for local protein synthesis indicate that the importance of post-transcriptional regulation extends beyond the cytoskeleton (Mili et al., 2008; Poon et al., 2006; Zivraj et al., 2010).

The post-transcriptional regulatory module elucidated in the current study fulfills many of the predictions made by the post-transcriptional operon model, which was inspired by high throughput studies showing that individual RNPs frequently associate with functionally inter-related RNAs (Keene, 2007; Keene and Tenenbaum, 2002). In this model, the fates of functionally inter-related transcripts are coordinated through the actions of shared trans-factors binding to structurally similar cis-elements on the RNAs, forming an RNA regulon, which co-regulates RNAs that might otherwise be transcribed differentially. The identification of multiple hnRNP K-associated transcripts that are upregulated with the onset of axon outgrowth, the presence of consensus RNA-binding sequences among them, and the demonstration that introducing a non-coding RNA bearing multiple copies of one of these sequences largely mimicked the effects of hnRNP K-knockdown on axon outgrowth and cytoskeletal organization are all supportive of such an RNA regulon having an essential role in axon outgrowth.

Large data sets generated by high throughput methods like RIP-chip have great potential for providing insights at the systems level, but their proper interpretation requires exercising some degree of caution. First, it would be inappropriate to conclude that all hnRNP K-targeted transcripts in *Xenopus* brain were successfully identified. We employed a fairly conservative selection criterion (fourfold enrichment) because we wanted to minimize interference from false positives for the purposes of testing a specific hypothesis (i.e. co-regulation of multiple cytoskeletal-associated transcripts). Being more stringent than that of other studies [e.g. twofold for
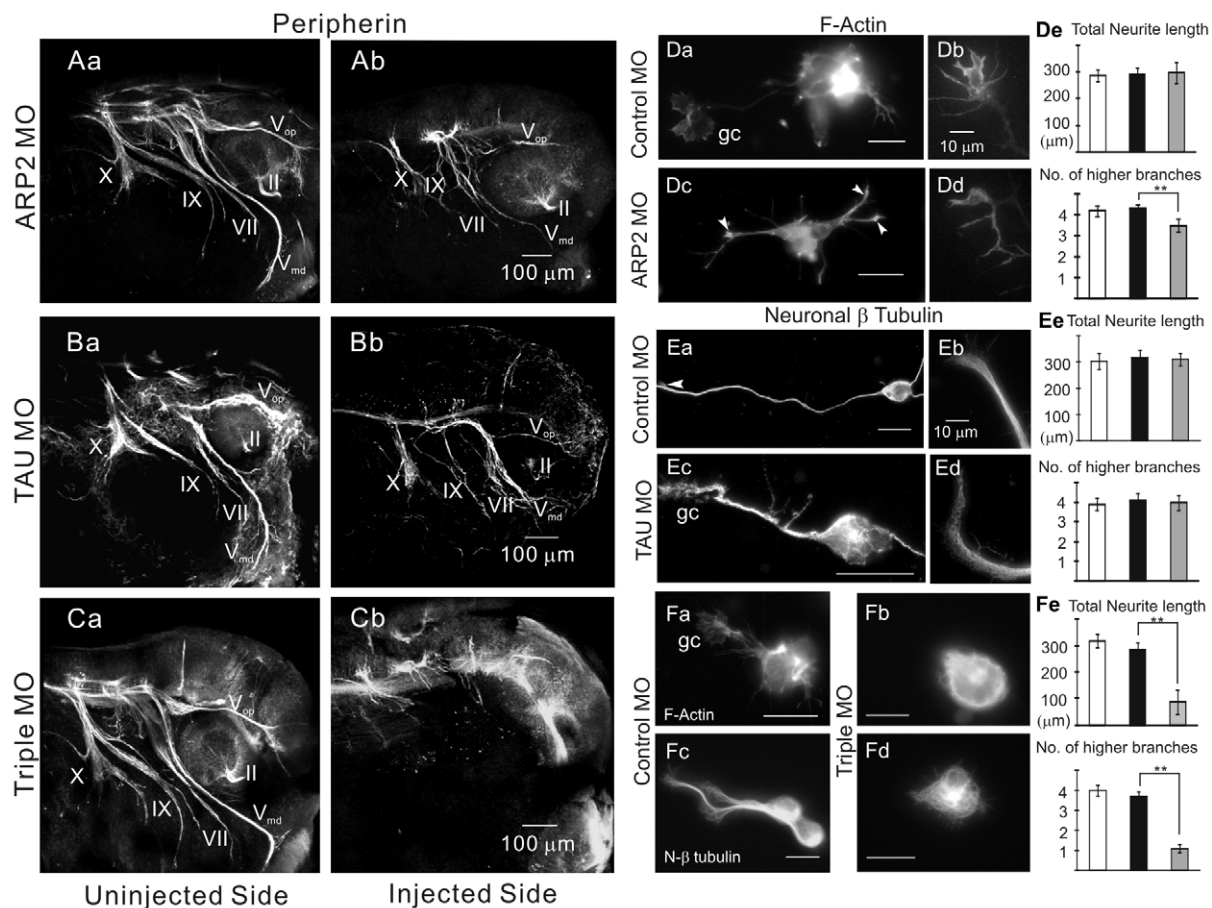
Fig. 8. Triple knockdown of Arp2, tau and XNIF substantially phenocopied hnRNP K knockdown. (**Aa-Cb**) Parasagittal optical sections of stage 37/38 heads immunostained for peripherin in whole mount. Whereas Arp2 MO (Aa,Ab) and tau MO (Ba,Bb) injected individually yielded only moderate defects in peripheral axon outgrowth on the injected side, triple knockdown of Arp2, tau and XNIF yielded severe defects (Ca,Cb). II, optic; V_{op} and V_{md}, opthalmic and mandibular branches of the trigeminal; VII, facial; IX, glossopharyngeal; and X, vagus nerves. (**Da-Fe**) In dissociated culture, Arp2 and tau MO injected individually yielded marked defects in actin filaments and microtubules, respectively, compared with control MO (Da-Dd, phalloidin stained; Ea-Ed, N-β tubulin immunostained). Triple knockdown of Arp2, tau and XNIF synergistically compromised axon outgrowth severely (Fb,Fd) compared with control MO (Fa,Fc). Fa,Fb, phalloidin stained; Fc,Fd, N-β tubulin immunostained. Scale bars: 100 μm for Aa-Cb; 10 μm for Db,Dd,Eb,Ed; 20 μm for Da,Dc,Ea,Ec,Fa-Fd. Bar graphs show mean total length of neuritic arbor and number of higher order branches (secondary and higher) per cell (±s.d., three cultures). White bars, uninjected; black bars, control MO-injected; gray bars, bilaterally injected with Arp2 (De), tau (Ee) or all three (Fe) MOs. **$P<0.01$, t-test. Numbers of uninjected, control MO and experimental MO neurons were: De: 128, 107, 106; Ee: 117, 104, 109; Fe: 108, 115, 126, respectively.

hnRNP E2 (Waggoner and Liebhaber, 2003)], it might, therefore, have rejected some bona fide hnRNP K-targeted transcripts. Second, owing to the relatively incomplete nature of the annotation of the *Xenopus laevis* genome (23%), we concentrated on the 130 genes that are fully annotated, although the entire data set is made available for future studies.

Although the significant defects in cytoskeletal polymer organization seen with hnRNP K-knockdown prompted us to focus on cytoskeletal-associated transcripts, the remaining array-identified transcripts might include additional components of the same hnRNP K RNA regulon as the three specific transcripts studied. After all, triple knockdown of cytoskeletal targets yielded many, but not all, defects observed with hnRNP K knockdown, such as filopodia formation. Although transcripts related to intracellular localization and transport, which represented the largest functional groups (37%), included the cytoskeletal-associated transcripts, others in this, and perhaps even additional groups, could conceivably be co-regulated by hnRNP K for axon

outgrowth. For example, within the transport group were identified five members of the RAS oncogene family (*RAB 1A*, *5A*, *6A*, *35* and *40C*), which mediate vesicle budding, motility and attachment to specific sites in the plasma membrane. RAB5 and RAB35 are already known to promote neurite outgrowth and branching (Chevallier et al., 2009; Satoh et al., 2008; Stenmark, 2009), and our polysomal profiling data indicated that *Rab5A* translation, like that of the cytoskeletal-associated transcripts, was reduced with hnRNP K knockdown, suggesting it, and perhaps other Rabs, might belong to the same hnRNP K RNA regulon as the cytoskeletal-associated transcripts.

RIP-chip-identified transcripts must also include ones belonging to other hnRNP K RNA regulons. This is partly a consequence of choosing juvenile brain as the source of mRNP complexes. Although it enabled us to sample a wide range of developmental states within a purely neural sample, it also undoubtedly captured transcripts involved in hnRNP K-mediated functions of neurons, and even glia, that are unrelated to axon outgrowth (Ji et al., 2011;

Yang et al., 2009). Indeed, translation of the transcription factors *Otx1* and *Pax6* was unaffected by hnRNP K knockdown (see Fig. S2 in the supplementary material), indicating that hnRNP K must be involved in some other mode of their regulation or at another time in development.

These latter findings are consistent both with hnRNP K being a multifunctional protein (Bomsztyk et al., 2004) and with the post-transcriptional operon model, in which an individual RNP combines with others to define larger regulons (Keene, 2007; Keene and Tenenbaum, 2002). Our study indicates that during neuronal development hnRNP K serves as an essential element of mRNP complexes that link together the post-transcriptional regulation of multiple RNAs whose proteins act jointly to form the axon. A substantial portion of these are proteins that integrate the separate cytoskeletal polymers into the arrangements that are both characteristic of and necessary for axon outgrowth. This study thus lays the foundation for future investigations into the regulation of these RNAs by hnRNP K, together with its associated kinases and participating RNPs, to yield new insights into the intrinsic molecular mechanisms controlling axon development.

Competing interests statement
The authors declare no competing financial interests.

Supplementary material
Supplementary material for this article is available at
http://dev.biologists.org/lookup/suppl/doi:10.1242/dev.066993/-/DC1

References

Adolph, D., Flach, N., Mueller, K., Ostareck, D. H. and Ostareck-Lederer, A. (2007). Deciphering the cross talk between hnRNP K and c-Src: the c-Src activation domain in hnRNP K is distinct from a second interaction site. *Mol. Cell. Biol.* **27**, 1758-1770.

Ananthakrishnan, L. and Szaro, B. G. (2009). Transcriptional and translational dynamics of light neurofilament subunit RNAs during *Xenopus laevis* optic nerve regeneration. *Brain Res.* **1250**, 27-40.

Ananthakrishnan, L., Gervasi, C. and Szaro, B. G. (2008). Dynamic regulation of middle neurofilament (NF-M) RNA pools during optic nerve regeneration. *Neuroscience* **153**, 144-153.

Baroni, T. E., Chittur, S. V., George, A. D. and Tenenbaum, S. A. (2008). Advances in RIP-chip analysis. *Methods Mol. Biol.* **419**, 93-108.

Benowitz, L. I., Shashoua, V. E. and Yoon, M. G. (1981). Specific changes in rapidly transported proteins during regeneration of the goldfish optic nerve. *J. Neurosci.* **1**, 419-426.

Blanchette, A. R., Fuentes Medel, Y. F. and Gardner, P. D. (2006). Cell-type-specific and developmental regulation of heterogeneous nuclear ribonucleoprotein K mRNA in the rat nervous system. *Gene Expr. Patterns* **6**, 596-606.

Bolstad, B. M., Irizarry, R. A., Astrand, M. and Speed, T. P. (2003). A comparison of normalization methods for high density oligonucleotide array data based on variance and bias. *Bioinformatics* **19**, 185-193.

Bomsztyk, K., Van Seuningen, I., Suzuki, H., Denisenko, O. and Ostrowski, J. (1997). Diverse molecular interactions of the hnRNP K protein. *FEBS Lett.* **403**, 113-115.

Bomsztyk, K., Denisenko, O. and Ostrowski, J. (2004). hnRNP K: one protein multiple processes. *BioEssays* **26**, 629-638.

Buchanan, J., Sun, Y. A. and Poo, M.-M. (1989). Studies of nerve-muscle interactions in *Xenopus* cell culture: fine structure of early functional contacts. *J. Neurosci.* **9**, 1540-1554.

Buckanovich, R. J., Posner, J. B. and Darnell, R. B. (1993). Nova, the paraneoplastic Ri antigen, is homologous to an RNA-binding protein and is specifically expressed in the developing motor system. *Neuron* **11**, 657-672.

Buckanovich, R. J., Yang, Y. Y. L. and Darnell, R. B. (1996). The onconeural antigen Nova-1 is a neuron-specific RNA-binding protein, the activity of which is inhibited by paraneoplastic antibodies. *J. Neurosci.* **16**, 1114-1122.

Campellone, K. G., Webb, N. J., Znameroski, E. A. and Welch, M. D. (2008). WHAMM is an Arp2/3 complex activator that binds microtubules and functions in ER to golgi transport. *Cell* **134**, 148-161.

Chevallier, J., Koop, C., Srivastava, A., Petrie, R. J., Lamarche-Vane, N. and Presley, J. F. (2009). Rab35 regulates neurite outgrowth and cell shape. *FEBS Lett.* **583**, 1096-1101.

Chow, I. and Poo, M.-M. (1985). Release of acetylcholine from embryonic neurons upon contact with muscle cell. *J. Neurosci.* **5**, 1076-1082.

Cleveland, D. W., Hwo, S.-Y. and Kirschner, M. W. (1977). Physical and chemical properties of purified tau factor and the role of tau in microtubule assembly. *J. Mol. Biol.* **116**, 227-247.

Collier, B., Goobar-Larsson, L., Sokolowski, M. and Schwartz, S. (1998). Translational inhibition in vitro of human papillomavirus type 16 L2 mRNA mediated through interactions with heterogeneous ribonucleoprotein K and poly(rC)-binding proteins 1 and 2. *J. Biol. Chem.* **273**, 22648-22656.

Dent, J. A., Polson, A. G. and Klymkowsky, M. W. (1989). A wholemount immunocytochemical analysis of the expression of the intermediate filament protein vimentin in *Xenopus*. *Development* **105**, 61-74.

Disanza, A. and Scita, G. (2008). Cytoskeletal regulation: coordinating actin and microtubule dynamics in membrane trafficking. *Curr. Biol.* **18**, R873-R875.

Dubey, M., Chaudhury, P., Kabiru, H. and Shea, T. B. (2008). Tau inhibits anterograde axonal transport and perturbs stability in growing axonal neurites in part by displacing kinesin cargo: neurofilaments attenuate tau-mediated neurite instability. *Cell Motil. Cytoskeleton* **65**, 88-99.

Farias, G. A., Muñoz, J. P., Garrido, J. and Maccioni, R. B. (2002). Tubulin, actin, and tau protein interactions and the study of their macromolecular assemblies. *J. Cell. Biochem.* **85**, 315-324.

Gagnon, M. L., Angerer, L. M. and Angerer, R. C. (1992). Posttranscriptional regulation of ectoderm-specific gene expression in early sea urchin embryos. *Development* **114**, 457-467.

Geisler, N., Kaufmann, E., Fischer, S., Plessmann, U. and Weber, K. (1983). Neurofilament architecture combines structural principles of intermediate filaments with carboxy-terminal extensions increasing in size between triplet proteins. *EMBO J.* **2**, 1295-1302.

Gervasi, C. and Szaro, B. G. (2004). Performing functional studies of *Xenopus laevis* intermediate filament proteins through injection of macromolecules into early embryos. *Methods Cell Biol.* **78**, 673-701.

Grant, S. and Keating, M. J. (1986). Ocular migration and the metamorphic and postmetamorphic maturation of the retinotectal system in *Xenopus laevis*: an autoradiographic and morphometric study. *J. Embryol. Exp. Morphol.* **92**, 43-69.

Habelhah, H., Shah, K., Huang, L., Ostareck-Lederer, A., Burlingame, A. L., Shokat, K. M., Hentze, M. W. and Ronai, Z. (2001). ERK phosphorylation drives cytoplasmic accumulation of hnRNP K and inhibition of mRNA translation. *Nat. Cell Biol.* **3**, 325-330.

Harada, A., Oguchi, K., Okabe, S., Kuno, J., Terada, S., Ohshima, T., Sato-Yoshitake, R., Takei, Y., Noda, T. and Hirokawa, N. (1994). Altered microtubule organization in small-calibre axons of mice lacking tau protein. *Nature* **369**, 488-491.

Hirokawa, N. and Takeda, S. (1999). Gene targeting studies begin to reveal the function of neurofilament proteins. *J. Cell Biol.* **143**, 1-4.

Hirokawa, N., Glicksman, M. A. and Willard, M. B. (1984). Organization of mammalian neurofilament polypeptides within the neuronal cytoskeleton. *J. Cell Biol.* **98**, 1523-1536.

Hirokawa, N., Shiomura, Y. and Okabe, S. (1988). Tau proteins: the molecular structure and mode of binding on microtubules. *J. Cell Biol.* **107**, 1449-1459.

Huang, D. W., Sherman, B. T. and Lempicki, R. A. (2009). Systematic and integrative analysis of large gene lists using DAVID bioinformatics resources. *Nat. Protoc.* **4**, 44-57.

Ingber, D. E. (2003). Tensegrity I. Cell structure and hierarchical systems biology. *J. Cell Sci.* **116**, 1157-1173.

Irwin, N., Baekelandt, V., Goritchenko, L. and Benowitz, L. I. (1997). Identification of two proteins that bind to a pyrimidine-rich sequence in the 3′-untranslated region of GAP-43 mRNA. *Nucleic Acids Res.* **25**, 1281-1288.

Ji, Y.-F., Xu, S.-M., Zhu, J., Wang, X.-X. and Shen, Y. (2011). Insulin increases glutamate transporter GLT1 in cultured astrocytes. *Biochem. Biophys. Res. Comm.* **405**, 691-696.

Keene, J. D. (2007). RNA regulons: coordination of post-transcriptional events. *Nat. Rev. Genet.* **8**, 533-543.

Keene, J. D. and Tenenbaum, S. A. (2002). Eukaryotic mRNPs may represent posttranscriptional operons. *Mol. Cell* **9**, 1161-1167.

Klimek-Tomczak, K., Wyrwicz, L. S., Jain, S., Bomsztyk, K. and Ostrowski, J. (2004). Characterization of hRNP K protein-RNA interactions. *J. Mol. Biol.* **342**, 265-278.

Lariviére, R. C. and Julien, J.-P. (2004). Functions of intermediate filaments in neuronal development and disease. *J. Neurobiol.* **58**, 131-148.

Leung, K.-M., van Horck, F. P. G., Lin, A. C., Allison, R., Standart, N. and Holt, C. E. (2006). Asymmetrical β-actin mRNA translation in growth cones mediates attractive turning to netrin-1. *Nat. Neurosci.* **9**, 1247-1256.

Lewis, H. A., Chen, H., Buckanovich, R. J., Yang, Y. Y., Musunuru, K., Zhong, R., Darnell, R. B. and Burley, S. K. (1999). Crystal structures of Nova-1 and Nova-2 K-homology RNA-binding domains. *Structure* **7**, 191-203.

Lin, H. and Schlaepfer, W. W. (2006). Role of neurofilament aggregation in motor neuron disease. *Ann. Neurol.* **60**, 399-406.

Lin, W. and Szaro, B. G. (1994). Maturation of neurites in mixed cultures of spinal cord neurons and muscle cells from *Xenopus laevis* embryos followed with antibodies to neurofilament proteins. *J. Neurobiol.* **25**, 1235-1248.

Lin, W. and Szaro, B. G. (1995). Neurofilaments help maintain normal morphologies and support elongation of neurites in *Xenopus laevis* cultured embryonic spinal cord neurons. *J. Neurosci.* **15**, 8331-8344.

Lin, W. and Szaro, B. G. (1996). Effects of intermediate filament disruption on the early development of the peripheral nervous system of *Xenopus laevis*. *Dev. Biol.* **179**, 197-211.

Liu, Y., Gervasi, C. and Szaro, B. G. (2008). A crucial role for hnRNP K in axon development in *Xenopus laevis*. *Development* **135**, 3125-3135.

Livak, K. J. and Schmittgen, T. D. (2001). Analysis of relative gene expression data using real-time quantitative PCR and the $2^{-\Delta\Delta CT}$ method. *Methods* **25**, 402-408.

Makeyev, A. V. and Liebhaber, S. A. (2002). The poly(C)-binding proteins: a multiplicity of functions and a search for mechanisms. *RNA* **8**, 265-278.

Mikula, M., Karczmarski, J., Dzwonek, A., Rubel, T., Hennig, W., Dadlez, M., Bujnicki, J. M., Bomsztyk, K. and Ostrowski, J. (2006). Casein kinases phosphorylate multiple residues spanning the entire hnRNP K length. *Biochim. Biophys. Acta* **1764**, 299-306.

Mili, S., Moissoglu, K. and Macara, I. G. (2008). Genome-wide screen reveals APC-associated RNAs enriched in cell protrusions. *Nature* **453**, 115-119.

Miyasaka, H., Okabe, S., Ishiguro, K., Uchida, T. and Hirokawa, N. (1993). Interaction of the tail domain of high molecular weight subunits of neurofilaments with the COOH-terminal region of tubulin and its regulation by τ protein kinase II. *J. Biol. Chem.* **268**, 22695-22702.

Moskowitz, P. F. and Oblinger, M. M. (1995). Transcriptional and post-transcriptional mechanisms regulating neurofilament and tubulin gene expression during normal development of the rat brain. *Mol. Brain Res.* **30**, 211-222.

Nakagawa, T. Y., Swanson, M. S., Wold, B. J. and Dreyfuss, G. (1986). Molecular cloning of cDNA for the nuclear ribonucleoprotein particle C proteins: a conserved gene family. *Proc. Natl. Acad. Sci. USA* **83**, 2007-2011.

Oschwald, R., Richter, K. and Grunz, H. (1991). Localization of a nervous system-specific class II β-tubulin gene in *Xenopus laevis* embryos by whole-mount in situ hybridization. *Int. J. Dev. Biol.* **35**, 399-405.

Ostareck, D. H., Ostareck-Lederer, A., Wilm, M., Thiele, B. J., Mann, M. and Hentze, M. W. (1997). mRNA silencing in erythroid differentiation: hnRNP K and hnRNP E1 regulate 15-lipoxygenase translation from the 3′ end. *Cell* **89**, 597-606.

Ostareck-Lederer, A., Ostareck, D. H. and Hentze, M. W. (1998). Cytoplasmic regulatory functions of the KH-domain proteins hnRNPs K and E1/E2. *TIBS* **23**, 409-411.

Ostareck-Lederer, A., Ostareck, D. H., Cans, C., Neubauer, G., Bomsztyk, K., Superti-Furga, G. and Hentze, M. W. (2002). c-Src-mediated phosphorylation of hnRNP K drives translational activation of specifically silenced mRNAs. *Mol. Cell. Biol.* **22**, 4535-4543.

Paziewska, A., Wyrwicz, L. S., Bujnicki, J. M., Bomsztyk, K. and Ostrowski, J. (2004). Cooperative binding of the hnRNP K three KH domains to mRNA targets. *FEBS Lett.* **577**, 134-140.

Poon, M. M., Choi, S. H., Jamieson, C. A., Geschwind, D. H. and Martin, K. C. (2006). Identification of process-localized mRNAs from cultured rodent hippocampal neurons. *J. Neurosci.* **26**, 3390-3399.

Satoh, D., Sato, D., Tsuyama, T., Saito, M., Ohkura, H., Rolls, M. M., Ishikawa, F. and Uemura, T. (2008). Spatial control of branching within dendritic arbors by dynein-dependent transport of Rab5-endosomes. *Nat. Cell Biol.* **10**, 1164-1171.

Schaeffer, E., Alder, J., Greengard, P. and Poo, M.-M. (1994). Synapsin IIa accelerates functional development of neuromuscular synapses. *Proc. Natl. Acad. Sci. USA* **91**, 3882-3886.

Schwartz, M. L., Shneidman, P. S., Bruce, J. and Schlaepfer, W. W. (1990). Axonal dependency of the postnatal upregulation in neurofilament expression. *J. Neurosci. Res.* **27**, 193-201.

Schwartz, M. L., Shneidman, P. S., Bruce, J. and Schlaepfer, W. W. (1992). Actinomycin prevents the destabilization of neurofilament mRNA in primary sensory neurons. *J. Biol. Chem.* **267**, 24596-24600.

Schwartz, M. L., Shneidman, P. S., Bruce, J. and Schlaepfer, W. W. (1994). Stabilization of neurofilament transcripts during postnatal development. *Mol. Brain Res.* **27**, 215-220.

Skene, J. H. P. and Willard, M. (1981). Changes in axonally transported proteins during axon regeneration in toad retinal ganglion cells. *J. Cell Biol.* **89**, 86-96.

Smith, A., Gervasi, C. and Szaro, B. G. (2006). Neurofilament content is correlated with branch length in developing collateral branches of *Xenopus* spinal cord neurons. *Neurosci. Lett.* **403**, 283-287.

Stenmark, H. (2009). Rab GTPases as coordinators of vesicle traffic. *Nat. Rev. Mol. Cell Biol.* **10**, 513-525.

Szaro, B. G. and Strong, M. J. (2010). Post-transcriptional control of neurofilaments: new roles in development, regeneration and neurodegenerative disease. *Trends Neurosci.* **33**, 27-37.

Szaro, B. G., Grant, P., Lee, V. M. Y. and Gainer, H. (1991). Inhibition of axonal development after injection of neurofilament antibodies into a *Xenopus laevis* embryo. *J. Comp. Neurol.* **308**, 576-585.

Tabti, N. and Poo, M.-M. (1991). Culturing spinal neurons and muscle cells from *Xenopus* embryos. In *Culturing Nerve Cells* (ed. G. Banker and K. Goslin), pp. 137-154. Cambridge: MIT Press.

Thisted, T., Lyakhov, D. L. and Liebhaber, S. A. (2001). Optimized RNA targets of two closely related triple KH domain proteins, heterogeneous nuclear ribonucleoprotein K and αCP-2KL, suggest distinct modes of RNA recognition. *J. Biol. Chem.* **276**, 17484-17496.

Thyagarajan, A. and Szaro, B. G. (2004). Phylogenetically conserved binding of specific KH domain proteins to the 3′ untranslated region of the vertebrate middle neurofilament mRNA. *J. Biol. Chem.* **279**, 49680-49688.

Thyagarajan, A. and Szaro, B. G. (2008). Dynamic endogenous association of neurofilament mRNAs with K-homology domain ribonucleoproteins in developing cerebral cortex. *Brain Res.* **1189**, 33-42.

Tint, I., Slaughter, T., Fischer, I. and Black, M. M. (1998). Acute inactivation of tau has no effect on dynamics of microtubules in growing axons of cultured sympathetic neurons. *J. Neurosci.* **18**, 8660-8673.

Tripathi, V., Ellis, J. D., Shen, Z., Song, D. Y., Pan, Q., Watt, A. T., Freier, S. M., Bennett, C. F., Sharma, A., Bubulya, P. A. et al. (2010). The nuclear-retained noncoding RNA MALAT1 regulates alternative splicing by modulating SR splicing factor phosphorylation. *Mol. Cell* **39**, 925-938.

Undamatla, J. and Szaro, B. G. (2001). Differential expression and localization of neuronal intermediate filament proteins within newly developing neurites in dissociated cultures of *Xenopus laevis* embryonic spinal cord. *Cell Motil. Cytoskeleton* **49**, 16-32.

Vize, P. D., Hemmati-Brivanlou, A., Harland, R. M. and Melton, D. A. (1991). Assays for gene function in developing *Xenopus* embryos. In *Xenopus laevis: Practical Uses in Cell and Molecular Biology* (ed. B. K. Kay and H. B. Peng), pp. 368-388. San Diego: Academic Press.

Waggoner, S. A. and Liebhaber, S. A. (2003). Identification of mRNAs associated with αCP2-containing RNP complexes. *Mol. Cell. Biol.* **23**, 7055-7067.

Walker, K. L., Yoo, H.-K., Undamatla, J. and Szaro, B. G. (2001). Loss of neurofilaments alters axonal growth dynamics. *J. Neurosci.* **21**, 9655-9666.

Weingarten, M. D., Lockwood, A. H., Hwo, S. Y. and Kirschner, M. W. (1975). A protein factor essential for microtubule assembly. *Proc. Natl. Acad. Sci. USA* **72**, 1858-1862.

Yang, Y., Gozen, O., Watkins, A., Lorenzini, I., Lepore, A., Gao, Y., Vidensky, S., Brennan, J., Poulsen, D., Park, J. W. et al. (2009). Presynaptic regulation of astroglial excitatory neurotransmitter transporter GLT1. *Neuron* **61**, 880-894.

Yao, J., Sasaki, Y., Wen, Z., Bassell, G. J. and Zheng, J. Q. (2006). An essential role for beta-actin mRNA localization and translation in Ca^{2+}-dependent growth cone guidance. *Nat. Neurosci.* **9**, 1265-1273.

Yoshimura, T., Arimura, N. and Kaibuchi, K. (2006). Signaling networks in neuronal polarization. *J. Neurosci.* **26**, 10626-10630.

Zivraj, K. H., Tung, Y. C., Piper, M., Gumy, L., Fawcett, J. W., Yeo, G. S. and Holt, C. E. (2010). Subcellular profiling reveals distinct and developmentally regulated repertoire of growth cone RNAs. *J. Neurosci.* **30**, 15464-15478.

Zuker, M. (2003). M-fold web server for nucleic acid folding and hybridization prediction. *Nucleic Acids Res.* **31**, 3406-3415.